Defence Science Journal, Vol. 59, No. 3, May 2009, pp. 284-293

RDX/AP-CMDB Propellants Containing Fullerenes and Carbon Black Additives

X. Han[1], T.F. Wang[1], Z.K. Lin[1], D.L. Han[1], S.F. Li[1], F.Q. Zhao[2], and L.Y. Zhang[2]

[1]*University of Science and Technology of China, Hefei, China, 230 026*
[2]*Xi'an Modern Chemistry Research Institute, Xi'an, China, 710 065*

ABSTRACT

The influence of fullerene additives on the combustion behaviour of cyclotrimethylene trinitramine/ammonium perchlorate composite modified double-base (RDX/AP-CMDB) propellants are investigated by thermogravimetric-differential thermogravimetric (TG-DTG) analysis, burning rate tests, and scanning electron microscopy observations. The difference between lead salicylate (Φ-*Pb*) and bismuth citrate acid (СП-*Bi*) as combustion modifiers has also been examined. TG-DTG investigations show that the addition of all additives advanced and accelerated the evaporation of nitroglycerin (NG). The addition of Extracted Fullerene Soot (EFS), C_{60} and carbon black (CB) additives obviously accelerated the liquid phase decomposition of NG. Also, the solid phase decomposition of nitrocellulose (NC) and the liquid phase decomposition of RDX were accelerated by 0.5 per cent Fullerene Soot (FS)/2.5 per cent СП-*Bi*/0.5 per cent copper adipic acid (J-*Cu*) composite catalyst. The addition of all composite catalysts promoted the decomposition of ammonium perchlorate (AP) except 0.5 per cent EFS/2.5 per cent СП-*Bi*/0.5 per cent J-Cu composite catalysts. It is well known that there exists dark zone in the flame structure of RDX-CMDB propellant, but in our observation, the dark zone vanished with the addition of 10 per cent AP to the forenamed propellant. The burning rates were increased at low pressure but reduced at high pressure by all catalysts except 0.5 per cent EFS/2.5 per cent СП-*Bi*/0.5 per cent J-*Cu* and 0.5 per cent C_{60}/2.5 per cent СП-*Bi*/0.5 per cent J-*Cu* which reduced the burning rates at every tested pressure. The pressure exponents of tested propellants were reduced by 0.5 per cent FS/2.5 per cent СП-*Bi*/0.5 per cent J-*Cu* with a factor of 17 per cent . The quenched surface observations significantly differed with the additions of diverse composite catalysts, which were consistent with the burning rate results.

Keywords: Fullerene, combustion properties, burning rate, CMDB propellant, RDX/AP-CMDB propellants

1. INTRODUCTION

Numerous experimental and theoretical investigations have been carried out on the combustion of nitramine solid propellant[1, 2]. Since RDX is an energetic material in RDX composite modified double-base (RDX-CMDB) propellant, it is used as a major oxidant of propellants and explosives. However, the main disadvantages of RDX-CMDB propellants are the existence of dark zone, high pressure exponent (*n*) value[3,4] and decrease in the burning rates with increase in the energy contained in the unit mass of the propellants. The dark zone in the flame structure of RDX-CMDB propellant vanishes with a small amount of ammonium perchlorate (AP) and this kind of propellant is labeled as RDX/AP-CMDB propellant. Also, a large number of experiments have been carried out to lower the pressure index of RDX-CMDB propellants by traditional burning rate catalysts such as lead salicylate, but these have met with the limited applications[5,6]. Research was carried out to incorporate the composite catalysts into RDX-CMDB propellants. Fullerenes are reported to be used as additives capable of increasing burning rates and lowering the concentration of NO_x in gas combustion products of RDX-CMDB propellants with incorporation of lead salts and copper salts modifiers[7,8]. Li[9], *et al.* reported that the fullerenes on the burning surface formed thermally stable Pb_xC_{60} active site through the microstructure observation of quenched surface in double base propellant with lead salt.

In this study, the effect of fullerene additives on the combustion behaviour of RDX/AP-CMDB propellants, which contained a RDX concentration of 20 per cent, AP concentration of 10 per cent ,were investigated by thermo-gravimetric-differential thermogravimetric (TG-DTG) analysis, burning rate tests, and scanning electron microscopy observations. The difference of lead salicylate (Φ-*Pb*) and bismuth citrate acid (СП-*Bi*) as combustion modifiers was also examined.

2. EXPERIMENTAL

2.1 Ingredients

To study the effect of fullerene additives on the combustion behaviour of RDX/AP-CMDB propellants and the difference of lead and bismuth salts as combustion modifiers, seven types of propellants (P-1~P-7) were prepared by rolling process. The detailed chemical ingredients of the reference propellants and burning rate catalysts are shown in Table 1 and 2. During this study, a sample consisting of 20 per cent RDX, 10 per cent AP, 29 per cent nitrocellulose

Received 18 June 2008

Table 1. Weight percentage of basic ingredients in the reference propellant

Ingredients	RDX	AP	NC	NG	Additives	Catalyst
Content (%)	20	10	29	32.5	5.0	3.5

Note: (i) The granularities of RDX are 80 μm and 50 μm with a weight ratio of 1:1; (ii) The granularity of AP is in the range of 120-200 μm; (iii) N % of NC is 12.6.

Table 2. Components of the burning rate catalysts (weight percentage)

Sample	CB	FS	EFS	C_{60}	Φ-*Pb*	СП-*Bi*	J-*Cu*
P-1	---	---	---	---	---	---	---
P-2	0.5	---	---	---	---	2.5	0.5
P-3	---	0.5	---	---	2.5	---	0.5
P-4	---	0.5	---	---	---	2.5	0.5
P-5	---	---	0.5	---	2.5	---	0.5
P-6	---	---	0.5	---	---	2.5	0.5
P-7	---	---	---	0.5	---	2.5	0.5

Note: (1) CB: carbon black; (2) FS: fullerene soot (comprised of 10% fullerenes and 90% carbon black); (3) EFS: extracted fullerene soot (contains about 80% C_{60} and 20% C_{70}); (4) Φ-*Pb*: phthalic acid lead; (5) СП-*Bi*: bismuth citrate acid; (6) J-*Cu*: adipic acid copper; (7) ---: without this component.

(NC) and 32.5 per cent nitroglycerin (NG) is made as a reference propellant. Other six types of RDX/AP-CMDB propellants were prepared by adding different ingredients of fullerene and CB burning rate catalysts to the reference propellant. The granularities of the RDX particles used are 80 μm and 50 μm with a weight ratio of 1:1. The granularity of AP was in the range of 120-200 μm and the *N* per cent of NC is 12.6.

2.2 TG-DTG Studies of RDX/AP-CMDB Propellants with Fullerenes Burning Rate Catalysts

TG-DTG curves were obtained by Shimadzu TGA-50 thermogravimetric instrument. The sample cup was aluminum oxide crucible and the temperature range employed was 30-600 °C with a heating rate of 10 °C/min. The shielding gas was high-pure nitrogen atmosphere with a purge rate of 25 ml/min. The sample mass was 3 mg in each run.

2.3 Burning rate tests

The dimension of each strand was 4×4 mm in cross section and 160 mm in length. The burning rates were measured by a conventional Crawford bomb with a coating and inhibition layer of the free surface of strands to enable a true cigarette burning behavior. The onset of propellant strands was ignited using electrically heated nichrome wire for various nitrogen pressures of 2, 4, 6, 8, 10, 12 and 14 Mpa with a constant initial temperature of 20 °C. Three parallel tests were made at each pressure to ensure the credibility of the experimental results.

2.4 SEM Observations of Quenched Surface of RDX/AP-CMDB Propellants with Additives

For the sake of investigating, the quenched surface of RDX/AP-CMDB propellants with fullerenes additives, the propellant is sliced into a slab with a dimension of 5×2×15 mm. The tested slabs without inhibitor were stuck on a stainless-steel plate. A nichrome wire with 0.3 mm dia was used for ignition, and it had a tight contact with the upper surface of the slab. Two transparent windows were designed in the opposite positions of the combustion chamber. This sealed combustion chamber was filled with 3.0 MPa N_2. The sample was ignited; then suddenly reducing the pressure and extinguishing the flame through proper control of the burning process, a plain quenched sample surface was obtained.

3. RESULTS AND DISCUSSION

3.1 Effects of Fullerenes Additives on Thermal Decomposition of RDX/AP-CMDB Propellants

When 3.0 mg samples were heated in Al_2O_3 pans without cover, the DTG curves recorded are shown in Figs 1 and 2. Melting of NG started even at about 50 °C and the decomposition rate was quickened with elevation in temperature. The peaks in the region of 139-146 °C belongs to adsorbed water and these processes should be weakly reflected in the TG curves.

The peaks at about 190-260 °C in the DTG curves of P-1 correspond to the decomposition of NG. These two peaks are coincident with the addition of 0.5 per cent EFS/2.5 per cent Φ-*Pb*/0.5 per cent J-*Cu*, 0.5 per cent EFS/2.5 per cent СП-*Bi*/0.5 per cent J-*Cu* and 0.5 per cent C_{60}/2.5 per cent СП-*Bi*/0.5 per cent J-*Cu* and disappeared with the addition of 0.5 per cent CB/2.5 per cent СП-*Bi*/0.5 per cent J-*Cu*. Due to the spherical structure of EFS and C_{60} in the composite catalysts, the decomposition products such as NO_2, H_2O and acid, etc were absorbed on the surface of NG, so the oxidation and hydrolysis reactions showed evidently to be auto-accelerated. The heats released from these reactions were accumulated in the condensed phase and this in turn accelerated the decomposition reactions. The addition of FS composite catalysts didn't affect the thermal decomposition of NG.

The peaks in the region of 190-260 °C belong to the

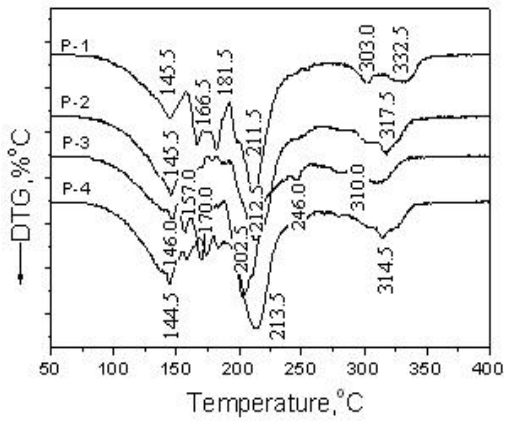

Figure 1. DTG curves of the tested propellants, P-1: reference propellant; P-2: with 0.5 per cent CB/ 2.5 per cent CП-*Bi*/0.5 per cent J-*Cu*; P-3: with 0.5 per cent FS/2.5 per cent Φ-*Pb*/0.5 per cent J-*Cu*; P-4: with 0.5 per cent FS/2.5 per cent CП-*Bi*/0.5 per cent J-*Cu*.

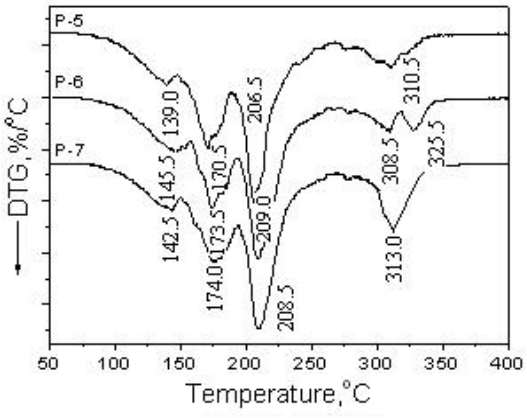

Figure 2. DTG curves of the tested propellant, P-5: with 0.5 per cent EFS/2.5 per cent Φ-*Pb*/0.5 per cent J-*Cu*; P-6: with 0.5 per cent EFS/2.5 per cent CП-*Bi*/0.5 per cent J-*Cu*; P-7: with 0.5 per cent C_{60}/2.5 per cent CП-*Bi*/0.5 per cent J-*Cu*.

solid phase decomposition of NC and liquid phase decomposition of RDX. The decomposition of NC starts with the rupture of *O-NO*$_2$ bond to form aldehyde-type compound, then the NO_2 reacts with the new born carboxyl and releases CO_2. Finally, remained nitrate bonds rupture. Thermal decomposition reaction of RDX is in first order and the gaseous phase decomposition products are N_2, N_2O, *NO*, *CO*, CO_2, etc. The liquid phase decomposition reaction of RDX is obviously an auto-catalysis reaction. Its first step is the rupture of *N*-heterocyclic and the second step is the release of NO_2 through radical decomposition reaction[10].

The solid phase decomposition of NC and liquid phase decomposition of RDX were slightly hastened with the addition of EFS and C_{60} additives, but these were almost uninfluenced by the addition of 0.5 per cent C*B*/2.5 per cent CП-*Bi*/0.5 per cent J-*Cu* and 0.5 per cent FS/2.5 per cent CП-*Bi*/0.5 per cent J-*Cu*. With the addition of 0.5 per cent FS/2.5 per cent Φ-*Pb*/0.5 per cent J-*Cu* composite catalysts, the solid phase decomposition of NC and liquid phase decomposition of RDX were evidently accelerated because the peak temperature of P-3 was lowered to 202.5 °C.

The peaks at temperature above 300 °C were corresponding to the decomposition of AP. From Figs 1 and 2 it could be seen that this process was dramatically accelerated with the addition of every composite catalyst except 0.5 per cent EFS/2.5 per cent CП-*Bi*/0.5 per cent J-*Cu*. There were two obvious peaks above 300 °C in the DTG curves of P-1 and two inconspicuous peaks in the DTG curves of P-6. These were corresponding to the low and high temperature decomposition of AP, respectively. Jacobs[11] reported that both the low and high temperature decomposition processes of AP were following the proton-transfer mechanism. At lower temperature, the main reaction is between NH_3 and $HClO_4$. Due to the imperfect oxidation of NH_3 by $HClO_4$, the remained NH_3 covers the entire surface of AP crystals and the low-temperature decomposition stops. Consequently, the low-temperature process usually terminates with a weight loss of 30 per cent . In the high-temperature decomposition process, the NH_3 and $HClO_4$ are released to gas phase from AP surface and $HClO_4$ further decomposes to oxidative products. NH_3 is oxidised by the oxidative products to form the terminal products. The low and high temperature peaks of AP were consistent with the addition of all catalysts except 0.5 per cent EFS/2.5 per cent CП-*Bi*/0.5 per cent J-*Cu*, and this showed that the addition of other five composite catalysts promoted the decomposition of AP.

3.2 Effects of 0.5 per cent Fullerenes/2.5 per cent CП-*Bi*/0.5 per cent J-*Cu* and 0.5 per cent CB/2.5 per cent CП-*Bi* /0.5 per cent J-*Cu* Additives on the Burning Rate Characteristics of RDX/AP-CMDB Propellants

It is well known that the burning rate of RDX-CMDB propellant decreases with increase in the concentration of RDX[12]. Also, the burning rate of RDX-CMDB propellant is independent of the particle size of RDX[13]. Due to the increase in the flame temperature, the specific impulse (I_{sp}) increases when RDX is mixed with CMDB propellants. Because of the fuel-rich RDX and double-base (DB) propellant, there is no endothermic reaction among the combustion products. The combustion reaction zone of RDX-CMDB propellant is similar to that of DB propellant and it is different from that of AP-CMDB propellant. The combustion wave structure of RDX-CMDB propellant is made up of fizz zone, dark zone, and second illuminate flame zone. The RDX crystal particle melts, decomposes, and vaporises on the burning surface of RDX-CMDB propellant. The gas products released from the decomposition of RDX diffuse to the decomposition gas of propellant bulk at the burning surface[12,14]. This diffused process occurs before the combustion of RDX particle at the propellant burning surface. Therefore, the homogeneous reactive gases mixed by the decomposition products of RDX crystal particles and propellant bulk are formed on the burning surface. Then, illuminate flame zone is formed at a certain distance above burning surface and the distance decreases with the enhancement of pressure.

In this research, all the samples have a constant RDX concentration of 20 per cent which is prepared by two granularities of 80 μm and 50 μm with a weight ratio of 1:1. The effects of different catalysts with 2.5 per cent СП-*Bi* and 0.5 per cent J-*Cu* additives on the burning rate characteristics of RDX/AP-CMDB propellants are shown in Table 3. The initial temperature was constant with 20 °C during the measurement of burning rates. As shown in Table 3, addition of 0.5 per cent FS/2.5 per cent СП-*Bi*/0.5 per cent J-*Cu* and 0.5 per cent CB/2.5 per cent СП-*Bi*/0.5 per cent J-Cu slightly increased the burning rates of RDX/AP-CMDB propellants at relatively low pressure (<6 MPa) and lowered that at high pressure (≥ 6MPa). The addition of 0.5 per cent EFS/2.5 per cent СП-*Bi*/0.5 per cent J-*Cu* and 0.5 per cent C_{60}/2.5 per cent СП-Bi / 0.5 per cent J-*Cu* reduced the burning rates of RDX/AP-CMDB propellants at every investigated pressure. The above results show that, to obtain lower burning rate, EFS/СП-*Bi*/J-*Cu* and C_{60}/СП-*Bi* /J-*Cu* composite catalysts can be added to the RDX/AP-CMDB propellants.

3.3 Effects of 0.5 per cent FS/2.5 per cent Φ-Pb/0.5 per cent J-Cu and 0.5 per cent EFS/2.5 per cent Φ-Pb/0.5 per cent J-Cu on the Burning Rate Characteristics of RDX/AP-CMDB Propellants

The difference of P-3 and P-4 propellants was using Φ-*Pb* instead of СП-*Bi* in the composition of composite catalysts. From the burning rate data shown Table 4, it was found that the burning rates of AP/RDX-CMDB propellants were enhanced when pressure not more than 10 MPa and lowered when pressure > 10 MPa by 0.5 per cent FS/2.5 per cent Φ-Pb/0.5 per cent J-*Cu*. Especially at 2 MPa, the burning rates of P-3 increased about 14 per cent wrt P-1. Also, the burning rates of P-5 were higher than that of P-1 at low pressure. This is possibly because at low pressure, Φ-*Pb* decomposes to lead monoxide (*PbO*) after the decomposition of the basic ingredients of CMDB propellants. *PbO* participates in the basic reactions which changes the burning rate of tested propellants.

Cai[15] put forward the reactions of *PbO* with *C* and with *CO* as:

$$PbO + C \rightarrow Pb + CO \quad (1)$$

$$PbO + CO \rightarrow Pb + CO_2 \quad (2)$$

During the combustion process of RDX/AP-CMDB propellants, *PbO* formed by the decomposition of Φ-*Pb* easily reacts with carbon contained in the deposit char and *CO* produced during the combustion of propellants. Eisenreich[16] reported that during the combustion process of lead burning rate catalyst, the liquid lead droplets could be observed at the top of the deposit char. At lower pressure, the lead salt catalysts increase the carbonaceous matter and enhance the deposit char layer on the burning surface. This is possibly because *PbO* makes intermediate decomposition products *HCHO*, *CHO* and $(CHO)_2$ changing their reaction path and they are split to form deposit char on the surface of the *PbO* particles. The FS additive along with deposit char has a considerable specific surface area needed for heterogeneous reaction. They are called carbonaceous matter and have a porous structure with lots of micro pores and particles on them. Also the existence of carbonaceous matter on the burning surface changes the reducing path of partial *NO* and the reducing site of *NO* moves from the high-temperature flame zone to low-temperature carbonaceous matter. The *NO* can be reduced in the site near the burning surface at lower pressure and

Table 3. Influence of fullerenes and CB additives composite with bismuth citrate acid/copper adipic acid combustion modifiers on the burning rate characteristics of RDX/AP CMDB propellants at different N_2 pressure at 20 °C

N_2 pressure (MPa)	2	4	6	8	10	12	14
Sample No	Burning rate/mms^{-1}						
P-1	3.71	5.88	7.87	10.23	12.02	14.30	16.42
P-2	3.96	6.10	7.82	9.74	11.74	13.57	15.34
P-4	3.76	5.88	7.82	9.90	11.74	13.63	15.84
P-6	3.50	5.76	7.55	9.36	11.39	13.52	15.38
P-7	3.57	5.72	7.49	9.49	11.45	13.46	15.43

Table 4. Effects of FS and EFS composite with phthalic acid lead/copper adipic acid combustion modifiers on the burning rate characteristics of RDX/AP-CMDB propellants with different N_2 pressure at 20 °C

N_2 pressure (MPa)	2	4	6	8	10	12	14
Sample No	Burning rate/mms^{-1}						
P-1	3.71	5.88	7.87	10.23	12.02	14.30	16.42
P-3	4.43	6.83	8.56	10.42	12.05	13.61	15.60
P-5	4.13	6.18	7.95	9.78	11.51	13.23	15.41

Table 5. Influence of phthalic acid lead and bismuth citrate acid as combustion modifiers

N_2 pressure (MPa)	2	4	6	8	10	12	14
Sample No.	Burning rate/mms^{-1}						
P-3	4.43	6.83	8.56	10.42	12.05	13.61	15.60
P-4	3.76	5.88	7.82	9.90	11.74	13.63	15.84
P-5	4.13	6.18	7.95	9.78	11.51	13.23	15.41
P-6	3.50	5.76	7.55	9.36	11.39	13.52	15.38

Table 6. Pressure exponents of RDX/AP CMDB propellants

Sample	P-1	P-2	P-3	P- 4	P-5	P-6	P-7
n	0.77	0.70	0.64	0.74	0.70	0.75	0.75

the reaction heats released from the reducing of *NO* are moved from the flame zone to the burning surface. As a result, the temperature distribution in whole reaction zone is changed. On the whole, the increment of burning rates with the addition of lead salt catalysts is mainly due to the improvement of temperature gradient in the fizz zone.

The pressure affects the amount and the covering ratio of deposit char by the temperature gradient in the fizz zone. As the pressure increases, the temperature gradient increases and the distance between the burning surface and reaction zone shortens, so the deposit char layer thickness becomes thin. The formation and growth chances of carbon nuclei decrease, thus the amount of deposit char decreases. The reaction heat released from reducing of NO is decreased and the increasing rate of burning rate is lowered. Only when the pressure is higher than a certain value, the increasing rate of burning rate decreases with the increment of the pressure. In our research, this value is about 10 MPa for P-3 and 6 MPa for P-5.

3.4 Influence and comparison of Ф-*Pb* and СП-*Bi* as Combustion Modifiers

The comparison of Ф-*Pb* and СП-*Bi* as combustion modifiers in RDX/AP-CMDB propellants is shown in Table 5. It is shown that using Ф-*Pb* instead of СП-*Bi* in the 0.5 per cent FS/2.5 per cent СП-*Bi*/0.5 per cent J-*Cu* and 0.5 per cent EFS/2.5 per cent СП-*Bi* /0.5 per cent J-*Cu* composite catalysts, the burning rates are obviously increased when pressure is no more than 12 MPa and slightly lowered when pressure is larger than 12 MPa.

It is shown that using Ф-*Pb* instead of СП-*Bi* in the FS/СП-*Bi*/J-*Cu* and EFS/СП-*Bi*/J-*Cu* composite, the combustion stability of RDX/AP-CMDB propellants increased and this is useful for the engineering applications.

3.5 Effects of Fullerene and CB Additives on Pressure Exponents of RDX/AP-CMDB Propellants

The pressure exponent *n* of the burning rate is defined by Vielie's function:

$$n = (\partial \ln r / \partial \ln p)_{T_0} \quad (3)$$

T_0 is the initial propellant temperature with a constant value of 20 °C. The pressure exponent is important to ensure the steady operation of solid propellant motor and is usually smaller than 1. In general, *n* of DB propellant without catalyst is in the range of 0.4-0.85 and that of AP-CMDB propellant is in the range of 0.2-0.65. The *n* of nitramine-CMDB is usually higher than that of AP-CMDB propellant. The *n* of tested propellants are shown in Table 6. In our research, *n* of RDX/AP-CMDB propellants without catalyst is about 0.77 in the pressure range tested. This value is between the pressure exponents of AP-CMDB propellant and RDX -CMDB propellant.

It must be noted that the pressure exponents for six composite catalysts are all lower than the *n* of P-1. Among them, RDX/AP-CMDB with 0.5 per cent FS/2.5 per cent СП-*Bi*/0.5 per cent J-*Cu* has the smallest *n* of about 0.64 which is about 17 per cent lower than that of the reference propellant. When FS is used instead of CB in the 0.5 per cent CB/2.5 per cent СП-*Bi*/0.5 per cent J-*Cu*, the pressure exponent is lowered by a factor of 8.6 per cent ; using FS instead of EFS and C_{60} in the fullerene/СП-*Bi*/J-*Cu*, the pressure exponents are found to be lower by a factor of 14.7 per cent. Comparing the pressure exponent of P-3 to P-4 and P-5 to P-6, one can find that using phthalic acid lead instead of bismuth citrate acid has obviously lowered the pressure exponents of RDX/AP-CMDB propellant. In our samples, using phthalic acid lead instead of bismuth citrate acid in FS/СП-*Bi*/J-*Cu* and EFS/СП-*Bi*/J-*Cu* composite catalysts, the pressure exponent is lowered by a factor of 13.5 per cent and 6.7 per cent, respectively.

3.6 Observations of Quenched Surface of RDX/AP-CMDB Propellants

Figure 3(a) is a representative view of P-1's SEM micrograph without any additive. There is only irregular plain and foam structure on it. Figures 3(b), 3(c) and 3(d) are the enlargement of different parts of the quenched surface of P-1. The plain part is corresponding to the homogenous phase matter composed with molten oxides and binder, and the foam part due to the coke coming from the burnt binder. From the micrograph of plain part with a magnification of 10000, one can see there are many RDX crystals which are at specific sites in the plain part, and

there are lots of vanished air bubbles just underneath them. The sizes of RDX crystals are in the range of 0.50-3.10 μm. Lots of holes ranging in 0.07-7.45 μm disperse on the surface of P-1 [Fig. 3(c)]. The white materials between plain and foam part are the crystals of AP and the particle granularities are in the range of 0.36-1.56 μm. It is well known that there exists a dark zone in the flame structure of RDX-CMDB propellants, but in our observations of the SEM photographs, 10 per cent AP makes the disappearance of the dark zone. The melt point of RDX is about 205 °C which is lower than that of AP, so in the quenched process AP is condensed earlier than RDX.

Addition of 0.5 per cent CB/2.5 per cent СП-*Bi*/0.5 per cent J-*Cu* makes the SEM micrographs of P-2 significantly different from that of P-1. The quenched surface of P-2 can also be divided into two different parts. The smooth part is the molten layer which is also composed of molten oxides and binder, but the foam part is different from that of P-1. It is made up of carbon framework with lots of small holes and RDX crystals. The sizes of the holes are in the range of 0.1-10 μm. The appearance of RDX in the foam layer is possibly because CB along with the deposit char provides cohesion cores for RDX. Fig. 4(c) shows the microcosmic structure of the foam layer with a magnification of 10000. There are lots of small ball-shaped particles which are corresponding to metal *Bi* and lots of small white particles which are due to RDX at the edge of the fumaroles. Also, some AP crystals irregularly disperse in the foam layer. From Fig. 4(d), one can find that the sizes of AP are much larger than those of RDX.

From Fig. 5, it can be seen that the quenched surface of P-3 is different from that of P-1. It is quite rough and filled with large fumaroles as shown in Figures 5(a). Figure 5(b) is the part enlargement of SEM photograph of P-3. In this figure, some gray balls are due to lead metal. From the burning rates analysis of P-2, one knows that the lead metal could form from the decomposition of lead salts. The edges of carbon framework are fully covered with RDX crystals and hardly can the black carbon framework be seen. Figures 4(c) and 4(d) show the microcosmic structure of the molten oxides and binder, and the RDX shows no specific crystal structure. It is interesting that there is no obvious AP crystal which can be seen in the SEM photographs of P-3. This is possibly because the composite catalysts promote the absorbance of AP in the binder, and in the quenched process, AP particle rimes at the quenched surface with a carbon core couldn't form the large crystal.

The SEM micrographs of quenched surface of P-4 are shown in Fig. 6. Using СП-*Bi* instead of Ф-*Pb* made the quenched surface of P-4 highly different from that of P-3. Several fumaroles and some of molten RDX were deposited on the planar quenched surface. The configuration of RDX crystal in P-4 is the same as that in P-3. Song[17], *et al.* reported that the СП-*Bi* could enhance the burning rates of DB propellants, but in the present research, the СП-*Bi* had no significant effect on the burning rates of tested propellants. This is possibly because the addition of RDX and AP to DB propellants inhibits the catalytic effect of СП-*Bi*. The luminous zone in Fig. 6(c) is due to the poor conductance of this zone, and the white strip-shaped materials are СП-*Bi* without decomposition. The FS catalysts and the molten RDX are near to СП-*Bi*. The RDX in Fig. 6(d) has no crystal structure and bonds with each other to form a melting layer.

Figure 7 shows that the quenched surface of P-5 is composed of the foam layer and melting layer. The foam

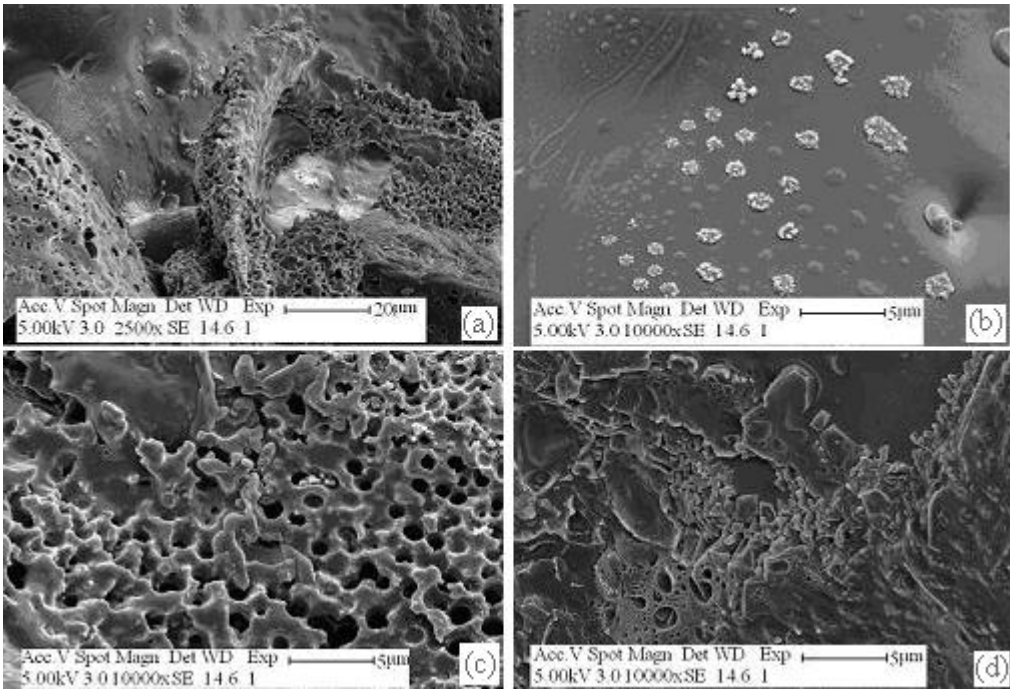

Figure 3. SEM micrographs of P-1: reference propellant.

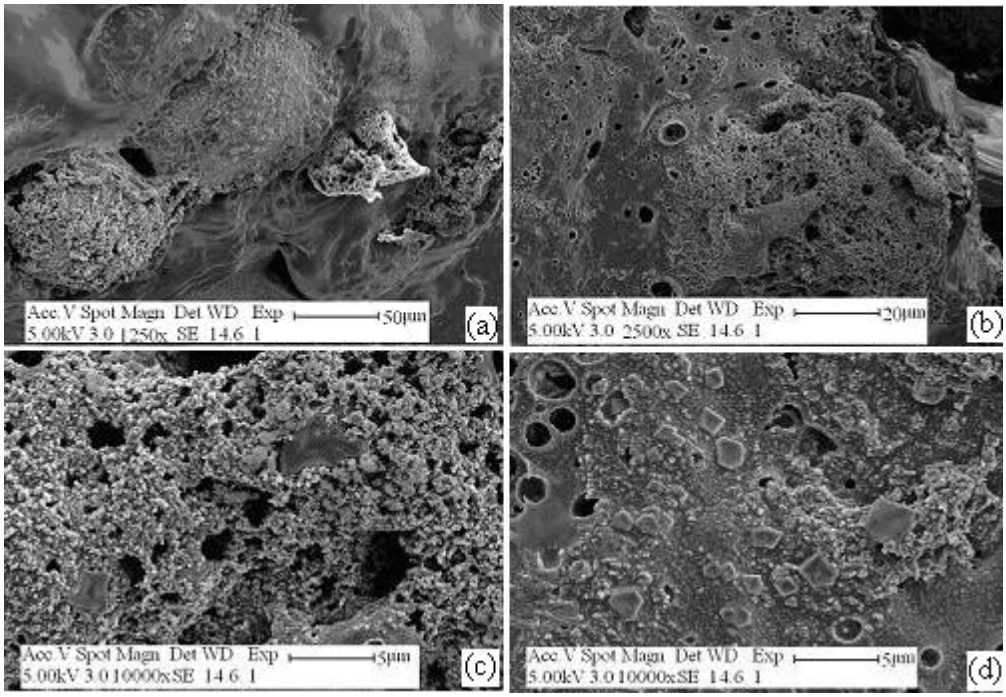

Figure 4. SEM micrographs of P-2: with 0.5 per cent CB/2.5 per cent CП-*Bi*/0.5 per cent J-*Cu* composite catalysts.

layer is mainly composed of carbon skeleton and crystallizing RDX. The sizes of fumaroles on the foam layer are smaller than those on the melting layer but the numbers are much larger than those on the melting layer. Figure 7(b) shows the enlarged view of the foam layer. From this micrograph, one can see that the foam layer is filled with fumaroles and RDX are crystallized at the edge of the holes. The formation of the fumaroles is attributed to the decomposition of oxides and binder. A part of RDX decomposes below the combustion surface, and the other part of RDX sublimates to the gas phase. In the quenched process, the decomposition of oxides and binder forms the fumaroles, and the coacervation of RDX forms the white substance at the edge of the fumaroles. The magnification shown in Fig. 7(b) is 20000 and that of Fig. 7(c) is 10000. The microstructure of melting layer is shown in Fig. 7(c). There are lots of small particles with nano-dimensions. The rodlike matters at the brim of these small particles are corresponding to lead oxides.

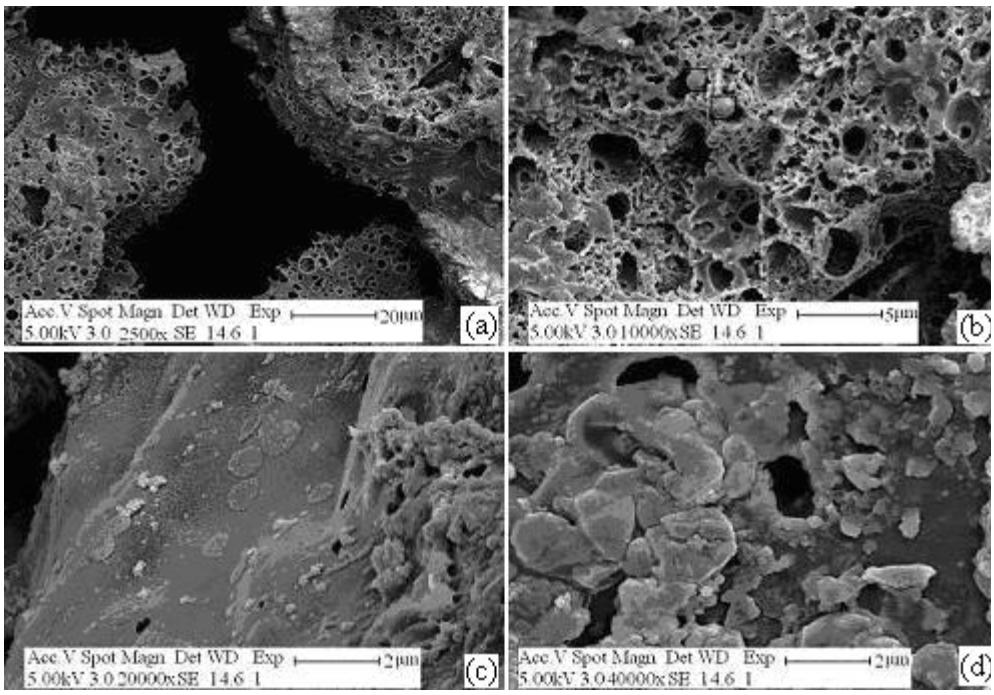

Figure 5. SEM micrographs of P-3: with 0.5 per cent FS/2.5 per cent Φ-*Pb*/0.5 per cent J-*Cu* composite catalysts.

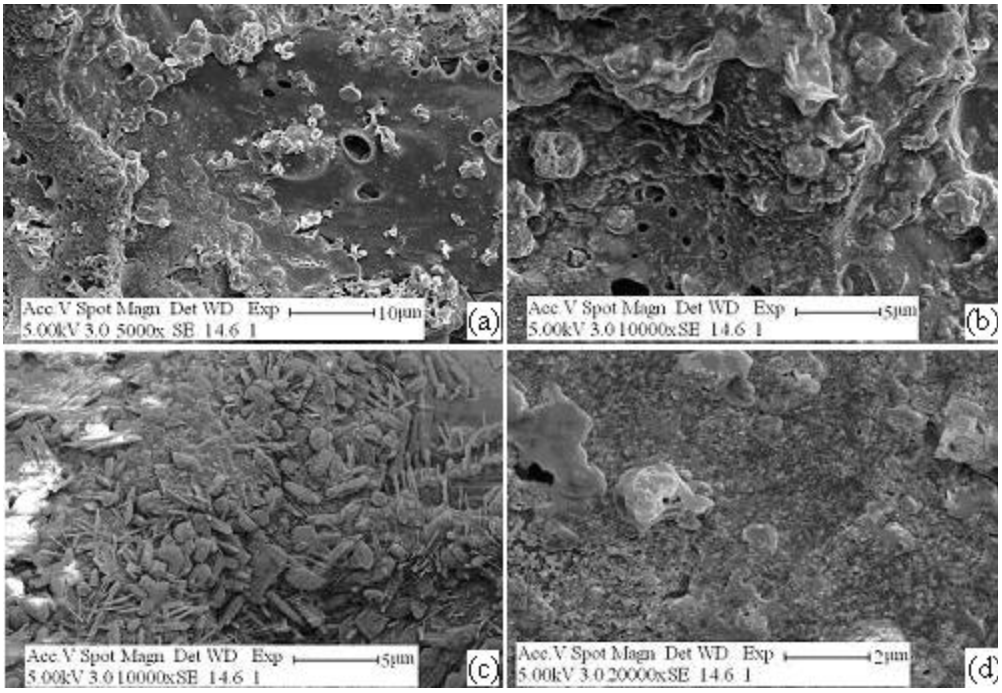

Figure 6. SEM micrographs of P-4: with 0.5 per cent FS/2.5 per cent CП-*Bi*/0.5 per cent J-*Cu* composite catalysts.

Figure 7(d) is the enlarged view of the *PbO*. This clearly shows the formation of *PbO* from the combination of small particles.

Figure 8 is the SEM photographs of P-6's quenched surface. At full view of this surface, it is relative plat and is composed mainly of melting layer. The lack of foam layer indicates that the combustion process is different from that of other propellants. The propellant combusts steadily at the entire surface and the oxides and binder decompose at the entire surface. RDX is crystallised at almost the entire surface of the melting layer. Figure 8(b) is microstructure of the catalysts part and it clearly shows that the sizes of the bismuth oxide are nano-dimension. Also, the bismuth oxides are discovered at the bottom of the fumaroles shown in Figs 8(c) and 8(d) displays the microstructure of RDX crystalline. The shape of RDX is quasiflake which is different from the pulverous shape in other propellants.

The quenched surface photographs of P-7 are shown in Fig. 9. There are lots of small particles on the surface

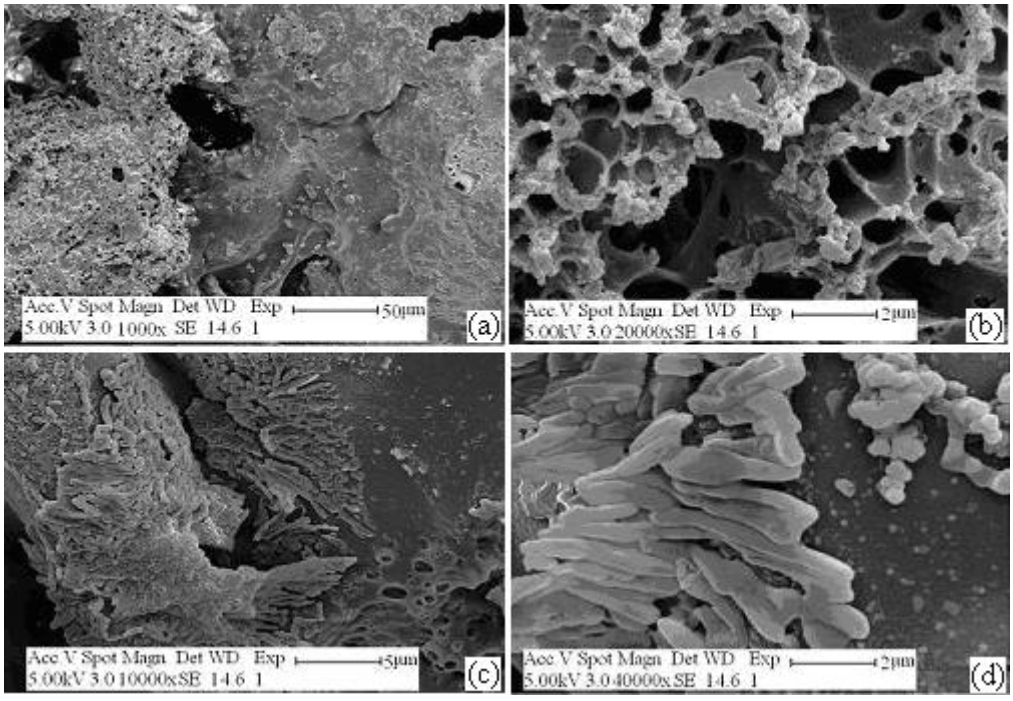

Figure 7. SEM micrographs of P-5: with 0.5 per cent EFS/2.5 per cent Φ-*Pb*/0.5 per cent J-*Cu* composite catalysts.

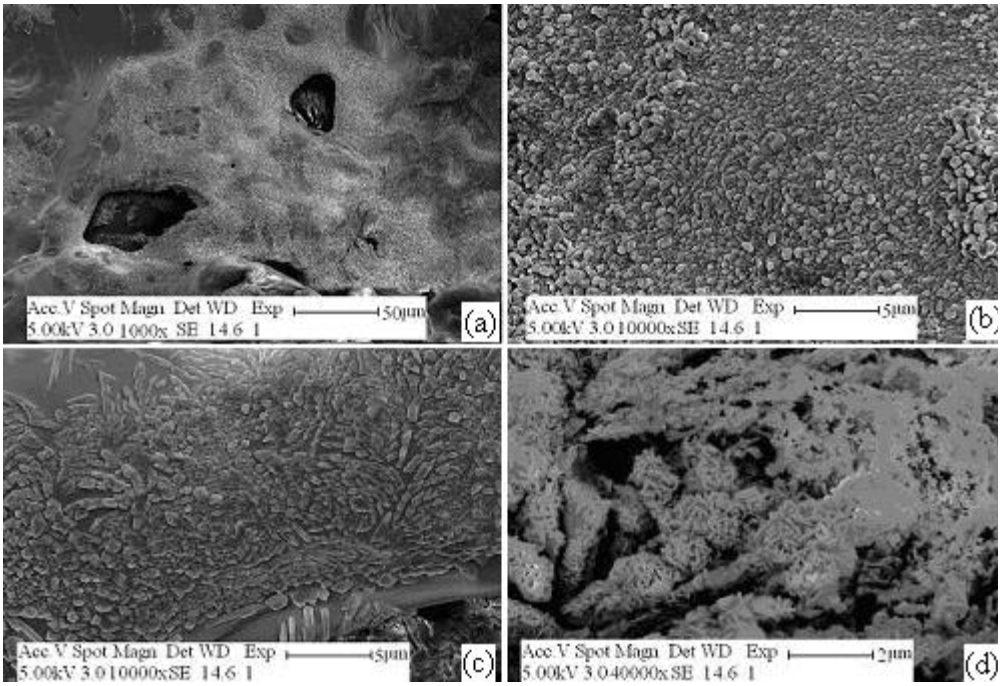

Figure 8. SEM micrographs of P-6: with 0.5 per cent EFS/2.5 per cent CП-*Bi*/0.5 per cent J-*Cu* composite catalysts.

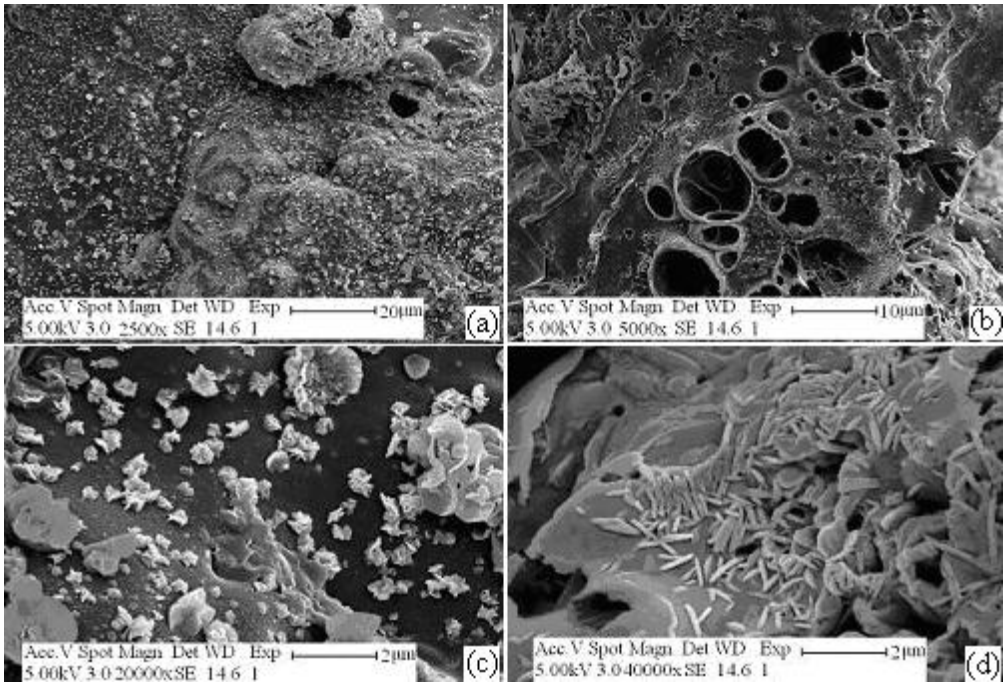

Figure 9. The SEM micrographs of P-7: with 0.5 per cent C_{60}/2.5 per cent CП-*Bi*/0.5 per cent J-*Cu* composite catalysts.

of the melting layer and only a few fumaroles are found in Figs 9(a). Figure 9(b) is the enlarged shape of the melting layer. The sizes of fumaroles are < 10 μm and hardly any catalyst is found on the surface of this zone. Figure 9(c) shows the microstructure of a small part of melting layer. From this photograph, one can find that the fine structures of RDX crystals are petaling shape. Some of these already grown up, and others under growth. Figure 9(d) shows the rodlike bismuth oxides dispersed on the surface of molten RDX. These bismuth oxides are in nano-dimension.

4. CONCLUSIONS

Analysis of TG-DTG results showed that the addition of all catalysts accelerated the evaporation of NG. The addition of EFS, C_{60} and CB additives obviously accelerated the liquid phase decomposition of NG. The addition of all composite catalysts promoted the decomposition of AP except 0.5 per cent EFS/2.5 per cent CП-*Bi*/0.5 per cent J-*Cu*. From the burning rate tests, one can see that the addition of 10 per cent AP makes the disappearance of dark zone in the flame structure of RDX-CMDB propellants.

The burning rates of RDX/AP-CMDB propellants were increased at low pressure but reduced at high pressure by every catalyst except 0.5 per cent EFS/2.5 per cent СП-*Bi*/0.5 per cent J-*Cu* and 0.5 per cent C_{60}/2.5 per cent СП-*Bi* /0.5 per cent J-*Cu* both of which reduced the burning rate at every tested pressure. The pressure exponents are lowered most by the addition of 0.5 per cent FS/2.5 per cent Φ-*Pb* /0.5 per cent J-*Cu* with a reducing pressure exponent of 17 per cent . Using FS instead of CB in the 0.5 per cent CB/2.5 per cent СП-*Bi* /0.5 per cent J-*Cu*, the pressure exponent is lowered by a factor of 8.6 per cent. While using FS instead of EFS and C_{60} in the fullerene/СП-*Bi*/J-*Cu*, the pressure exponents are lowered by a factor of 14.7 per cent . Also using phthalic acid lead instead of bismuth citrate acid in FS/СП-*Bi*/J-*Cu* and EFS/СП-*Bi*/J-*Cu* composite catalysts, the pressure exponent is lowered by a factor of 13.5 per cent and 6.7 per cent respectively. The quenched surface photographs differ significantly, indicating that the combustion process of the propellants studied also differ greatly.

ACKNOWLEDGEMENTS

The authors gratefully acknowledge financial support for this work by the National Natural Science Foundation of China (No.50476025). They also thank Z.R. Liu, X.N. Ren, H.X. Gao and J.H. Yi for fruitful discussions of the work as it progressed.

REFERENCES

1. Kubota, N. Role of additives in combustion waves and effect on stable combustion limit of double-base propellants. *Propell. Explos. Pyrot.*, 1978, **3**(6), 163-68.
2. Maruizumi, H.; Fukuma, D.; Shirota, K. & Kubota, N. Thermal decomposition of RDX composite propellants. *Propell. Explos. Pyrot.*, 1982. **7**(2). 40-45.
3. Cohen-Nir, E. Combustion characteristics of advanced nitramine-based propellants. *In* 18th Symposium (International) on Combustion, The Combustion Institute, Pittsburgh, Pa. 1981. pp. 195-206.
4. Kubota, N. Combustion mechanisms of nitramine composite propellants. *In* 18th Symposium (International) on Combustion, The Combustion Institute, Pittsburgh, Pa. 1981. pp.187-194.
5. Raman, K.V. & Singh, H. Ballistic modification of RDX-based CMDB propellants. *Propell. Explos. Pyrot.*, 1988. **13**(5), 149- 51.
6. Asthana, S.N.; Vaidya, M.V.; Shrotri, P.G. & Singh, H. Studies on minimum-signature-nitramine based high energy propellant. *J.Energ. Mater.*,1992. **10**(1), 1-16.
7. Zhao, F.Q.; Li, S.W.; Shan, W.G. & Li, S.F. Influence of C_{60}, fullerene-soot and carbon black on combustion properties of catalysed RDX-CMDB propellants. *J. Propu. Tech.*, 2000, **21**(2), 72-76.(in chinese).
8. Zhao, F.Q.; Li, S.W.; Chen, P.; Li, S.F. & He, D.Q. Effects of C_{60}, fullerene soot and carbon black on thermal decomposition of RDX-CMDB propellants, *J. Solid. Rock. Tech.*, 2000, **23**(2), 39-43.(in chinese).
9. Li, S.F. The microstructure observation of quenched surface in double-base propellant with lead salt. *Combust. Sci. Tech.*, 1998, **133**, 395-401.
10. Quintana, J.R.; Ciller, J.A. & Serna, F.J. Thermal behaviour of HMX/RDX mixtures. *Propell. Explos. Pyrot.*, 1992, **17**(3), 106-09.
11. Jacobs, R.V. & Russel-Jones, A.A. On the mechanism of decomposition of ammonium perchlorate. *Raketnaya Tekhnika i Kosmotavtika,* 1967, **5**(4), 275-78, (in Russian).
12. Kubota, N. & Masamoto, T. Flame structures and burning rate characteristics of CMDB propellants. *In* 16th Symposium (International) on Combustion, the Combustion Institute, Pittsburgh, Pa., 1976, pp. 1202-209.
13. Kubota, N., Fundamentals of solid propellant combustion, *In* Progress in Aeronautics and Astronautics. Kuo, K.K., Summerfield, M.(Eds.), *AIAA*. 1984, **90**.
14. Musso, R.C. & Grigor, A.F. Decomposition studies of propellant ingredients and ingredient combinations. *AIAA*, 1968, 468-95.
15. Cai, Y.F. Combustion mechanism of double-base propellants with lead burning rate catalysts. *Propell. Explos. Pyrotech.*, 1987, **12**(6), 209-14.
16. Eisenreich, N. A photographic study of the combustion zones of burning double base propellant strands. *Propell. Explos. Pyrotech.*, 1978. **3**(5), 141-46.
17. Song, X.D.; Zhao, F.Q.; Liu, Z.R.; Pan, Q. & Luo, Y. Thermal decomposition mechanism, non-isothermal reaction kinetics of bismuth citrate and its catalytic effect on combustion of double-base propellant. *Chem. J. Chin. Univer.*, 2006, **27**(1), 125-28.

Contributors

Mr X. Han is a Doctorate student in the Department of Chemical Physics, University of Science and Technology of China (USTC). He is working in the field of combustion chemistry.

Prof Shufen Li is a Professor in the Department of Chemical Physics at USTC. Her research area is combustion chemistry. She has served as the Director of the Laboratory of Combustion Chemistry of USTC. She is an Adjunct Professor at the National Key Laboratory. She is the Editor of *Chinese Journal of Explosives & Propellant, Journal of Solid Rocket Technology, and Energetic Materials*. She has published more than 170 research papers in national/international journals.